Journal of Alloys and Compounds 502 (2010) 54–58

Contents lists available at ScienceDirect

Journal of Alloys and Compounds

journal homepage: www.elsevier.com/locate/jallcom

Temperature dependence of critical stress and pseudoelasticity in a Fe–Mn–Si–Cr pre-rolled alloy

A. Baruj[a,b,*], G. Bertolino[a,b], H.E. Troiani[a,b]

[a] Centro Atómico Bariloche and Instituto Balseiro, Comisión Nacional de Energía Atómica (CNEA), 8400 San Carlos de Bariloche, Río Negro, Argentina
[b] CONICET, Argentina

ARTICLE INFO

Article history:
Received 8 March 2010
Received in revised form 6 April 2010
Accepted 7 April 2010
Available online 22 April 2010

Keywords:
Shape memory alloys (SMA)
Rolling
Thermomechanical processing
Transmission electron microscopy (TEM)
Mechanical properties testing

ABSTRACT

In this work, the mechanical behavior of Fe–28Mn–6Si–5Cr (wt.%) shape memory alloy subjected to a simple thermomechanical treatment consisting in rolling at 600 °C and subsequent aging at 800 °C for 10 min is studied. Martensite can be stress-induced in this material up to 110 °C. No stress-induced martensite was detected at temperatures above 150 °C. Extrapolating the mechanical testing data a yield stress for the austenite at room temperature σ_y = 450 MPa was calculated. In addition, a relatively large pseudoelastic behavior was observed at the temperature range between 90 and 110 °C. This effect is discussed on the basis of the formation of stacking faults and the reversible movement of their associated partial dislocations.

1. Introduction

The possibility of using shape memory steels based on the Fe–Mn system in structural applications has been proposed several years ago [1,2]. They would offer the advantages of a lower cost of production, ease of forming processes and large resistance to aggressive environments [2–4] in comparison to NiTi and Cu–Zn-based shape memory alloys (SMAs). However, this possibility was delayed by the need of performing a difficult and expensive thermomechanical treatment, the so-called "training", in order to achieve a useful shape memory effect (SME) in these materials [1]. In general, the SME of Fe–Mn-based alloys is related to a martensitic transformation between a fcc phase (austenite) and an hcp phase (martensite) [5–7]. Martensite is induced at room temperature by applying stress on the material and subsequently reversed by heating it up to a sufficiently high temperature. This process results in a large SME only if the reverse transformation proceeded by reversing the atomic path followed by the forward transformation [8,9]. Training consists in performing several cycles of stress-induced transformation followed by temperature-induced retransformation. Understandably, the associated costs of such a procedure are prohibitive.

Later on, by the beginning of 2000, newer Fe–Mn-based materials [10,11] and simpler thermomechanical processes were developed [12,13] overcoming the difficulties posed by the need of training. In particular, it has been recently found that Fe–Mn–Si–Cr alloys subjected to simple thermomechanical processing display a nearly full SME without the need of performing training [12,13]. For example, Fe–28Mn–6Si–5Cr rolled at 600 °C and annealed at 800 °C for 10 min recovers 95% of a 4% deformation previously introduced at room temperature [12]. Today, this material is one of the most promising candidates among Fe–Mn-based SMAs for real applications.

Although the material has been the subject of several publications in the past [14], most of them were related to the research of an optimum training treatment. There are almost no mechanical properties studies involving the material optimized by the newly developed thermomechanical treatment. For example, the literature contains no information about important parameters like the variation of the critical stress with the temperature, the room temperature yield stress (σ_y) or the limit temperature for the stress induction of martensite (M_d). Gathering data about these parameters could lead to a better understanding of the SME in this material and to optimize the thermomechanical treatment. Moreover, this lack of information hinders the design and dimensioning of applications.

In this paper, we present an experimental study of the mechanical properties of Fe–28Mn–6Si–5Cr rolled at 600 °C and annealed at 800 °C displaying almost perfect SME without training. We paid special attention to the temperature related behavior variations while reporting the critical parameters for this material.

* Corresponding author at: Centro Atómico Bariloche and Instituto Balseiro, Comisión Nacional de Energía Atómica (CNEA), 8400 San Carlos de Bariloche, Río Negro, Argentina. Tel.: +54 2944 445278; fax: +54 2944 445299.
E-mail address: baruj@cab.cnea.gov.ar (A. Baruj).

0925-8388/$ – see front matter © 2010 Elsevier B.V. All rights reserved.
doi:10.1016/j.jallcom.2010.04.123

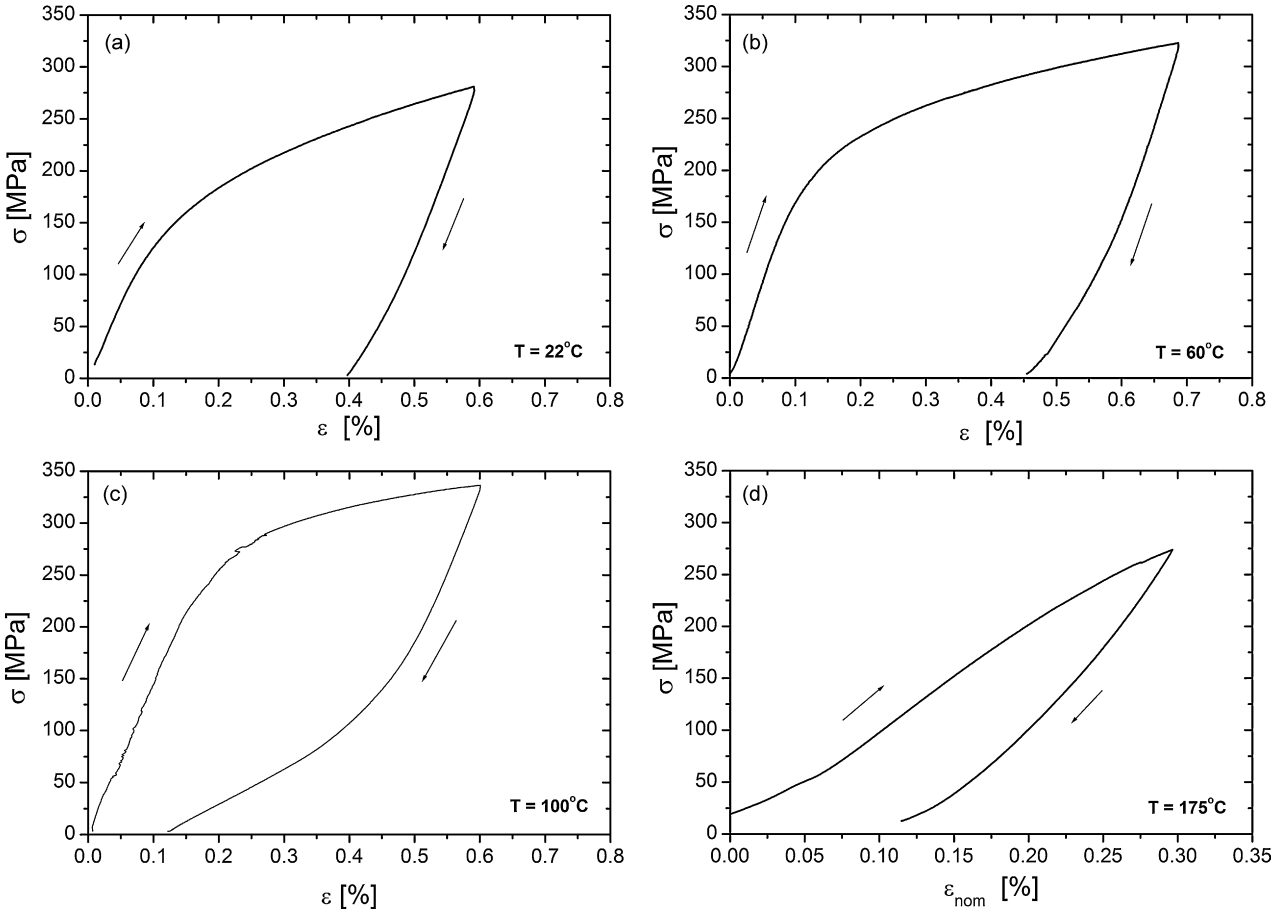

Fig. 1. Representative tensile stress–strain curves of pre-rolled Fe–28Mn–6Si–5Cr samples at different temperatures. An extensometer was used for measuring the deformation from room temperature up to 120 °C. (a) Room temperature. (b) 60 °C. (c) 100 °C, pseudoelastic behavior becomes apparent on the unloading part of the test. (d) 175 °C, the nominal deformation was calculated using the crosshead position in this case.

2. Experimental

In order to study the material, pure elements were induction-melted under Ar atmosphere to prepare an Fe–28Mn–6Si–5Cr (wt.%) 2 kg ingot. The ingot was solution treated at 1000 °C for 2 h and water quenched. Square-pillar shaped pieces of 100 mm × 20 mm × 16 mm were cut from the ingot and hot-rolled at 1055 °C to 11 mm thickness. The material was further rolled applying 20% thickness reduction at 600 °C. Cylindrical tensile test samples of 5 mm width and 25 mm gauge length were machined from the pre-rolled material and carefully polished in order to remove the surface layer. The samples were then enclosed in quartz capsules under Ar atmosphere, subjected to ageing at 800 °C for 10 min and water quenched. In a previous contribution, it was shown that the combination of rolling at 600 °C and ageing at 800 °C produced a large SME in this alloy without the need of performing a training treatment [12]. Tensile tests at different temperatures were performed in an Instron 5567 mechanical testing device at 0.1 mm/min constant speed. The testing machine has an attached temperature chamber (Instron 2119-005 TC) which allows performing tests up to 250 °C. In addition to the temperature chamber internal sensor, an Omega Type-K thermocouple with electronic cold juncture compensation was used to have a more precise measurement of the sample temperature. All tests were started 1 h after the reading of both temperature sensors stabilized. The temperature remained constant during each test. A MTS 632 axial extensometer was used for measuring the applied strain in the tests performed between 20 and 120 °C, while the position of the crosshead was used to calculate the deformation when the test temperature was higher. The critical stress was measured from stress–strain curves using the so-called 0.2% criterion, as stated by the ASTM-E8M standard. Martensitic transformation temperatures were determined by using a dilatometer designed and built in our laboratory. The pre-rolled material has a martensite start temperature $M_s = -25$ °C and a retransformation temperature $A_s = 120$ °C. Samples for transmission electron microscopy (TEM) observations were prepared directly from tensile test samples. Thin slices (about 0.5 mm) were cut by means of spark erosion and subsequently thinned down to 0.2 mm by applying a chemical polishing procedure. Then, discs of approximately 3 mm diameter were obtained by masking the slices and applying a suitable chemical solution (90 vol.% H_2O_2 + 5 vol.% HF + 5 vol.% HNO_3). As a result, these TEM samples were never mechanically polished, ensuring in this way the observation of defects or phases only introduced during mechanical testing. Finally, the discs were electropolished using a double jet with an acetic/perchloric 95:5 solution. The samples were observed in a Philips CM200 TEM with an accelerating voltage of 200 kV and ultratwin objective lens. Bright field (BF) and dark field (DF) images were acquired using a CCD camera and computer software while the microscope regular photo camera was used for recording the corresponding selected area diffraction patterns (SAD).

3. Results and discussion

The mechanical behavior of samples changes with the temperature. At room temperature (Fig. 1a) the stress–strain curve deviates from the initial linear elastic regime at the point where martensite starts to form in the material [15]. As it is usually observed in Fe–Mn–Si-based alloys, the transformation does not take place at a constant stress, i.e. there is no flat transformation plateau as it happens in the case, for example, of NiTi alloys. Instead, it is necessary to increase the stress to further proceed with the transformation. The critical stress corresponding to 0.2% applied strain is $\sigma_c(22\,^\circ\text{C}) = 235$ MPa. Upon unloading, the stress decreases almost linearly.

A similar behavior is observed as the temperature is increased. Fig. 1b and c show the results obtained at 60 and 100 °C, respectively. The main differences among the room temperature and these higher temperature tests are that the transformation stresses increase and that the curves strongly deviate from linearity upon unloading. This later feature is related with a pseudoelastic behavior, which has already been reported for this alloy subjected to a different thermomechanical treatment [16–17] and for a similar alloy containing NbC precipitates [18]. This effect is clearly

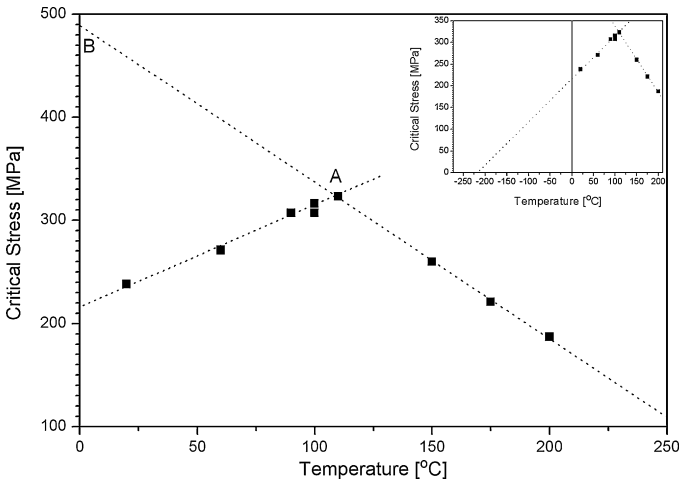

Fig. 2. Critical stress as a function of the temperature for pre-rolled Fe–28Mn–6Si–5Cr samples. Each point was measured using an individual sample. Straight lines result from the least-squares interpolation of the first three data on each side of the graph. Point A represents the intersection of both lines. Point B is the extrapolation of the plastic deformation line to 0 °C, at about 490 MPa. The inset corresponds to the same set of data but showing the extrapolation of the martensite induction line to 0 MPa, at about −220 °C.

observed at 100 °C where, apart from the standard elastic recovery, about 80% of the maximum applied deformation was pseudoelastically recovered after unloading.

Fig. 1d shows the result of the test performed at 150 °C. In the test shown in Fig. 1d and in tests performed at higher temperatures, the deformation was measured using the position of the crosshead because the extensometer could not stand temperatures above 120 °C, as explained in Section 2. In this temperature range, the critical stress decreases as the temperature increases and the pseudoelastic behavior was not observed.

The critical stresses measured in tensile experiments at different temperatures are summarized in Fig. 2. In experiments around room temperature, the critical stress is associated with the formation of stress-induced martensite. As the temperature increases, austenite is stabilized and consequently, the transformation stress increases. On the other hand, at temperatures of 150 °C and above, the critical stress corresponds to the yield stress of the material, which tends to decrease as the temperature increases. By performing a least-squares interpolation of the first three data on each side of Fig. 2, two straight lines were constructed. The intersection of both lines, denoted as point A in Fig. 2, defines two regions. On the left side of point A, the prevalent deformation mechanism is the stress-induced fcc to hcp martensitic transformation while on the right side prevails the introduction of irrecoverable slip. However, as a pronounced pseudoelastic effect was observed in the sample near to point A and martensite was detected in it in TEM observations, it is clear that this point does not mark the limit temperature for martensite formation. In the present experiments, the limit temperature M_d is in the range between 110 and 150 °C. There was no detectable pseudoelastic recovery in the tests performed at 150 °C and above. Point B in Fig. 2 marks the intersection of the linear extrapolation of the plastic deformation line to 0 °C. Considering this linear variation of the yield stress, a value of σ_y = 450 MPa can be calculated for the austenite at room temperature. The inset in Fig. 2 corresponds to the same set of data but showing the extrapolation of the martensite start line to 0 MPa. It crosses the x-axis at about −220 °C. This temperature is far below the measured M_s for this material, an indication of the non-thermoelastic character of its stress-induced martensitic transformation.

The remarkable pseudoelastic behavior displayed by the material at 100 °C was further analyzed by performing additional tests, including series of loading–unloading cycles at selected strain levels. The results are presented in Fig. 3a. During the first loading stage, the applied strain was ε = 0.3%, in coincidence with the result presented in Fig. 1c. At this strain level, the sample was repeatedly unloaded and loaded. A more detailed view of these cycles is presented in the inset of Fig. 3b. The cycles are almost closed, in each of them about 80% of the maximum deformation has been recovered. It is then remarkable that, under these conditions, the material has a repeatable pseudoelastic behavior. Nevertheless, a careful observation of the cycles reveals that they are not completely closed, meaning that the material does not return to exactly the same condition after each cycle. The small difference observed in each cycle is probably due to the combined introduction of very small amounts of stress-induced martensite and plastic deformation. When the strain is increased to ε = 1.0%, again almost closed unloading–loading cycles were obtained. Although the pseudoelastic component increases considered in absolute terms, it decreases in relation to the total deformation of the sample. Similar results were obtained as the strain level was increased to 2.0%, 3.0% and 4.0%.

TEM observation of samples deformed at 100 °C revealed the presence of thin martensite plates at some places of each grain, accompanied by a large density of isolated stacking faults and a few scattered dislocations. Fig. 4a shows an example of this microstruc-

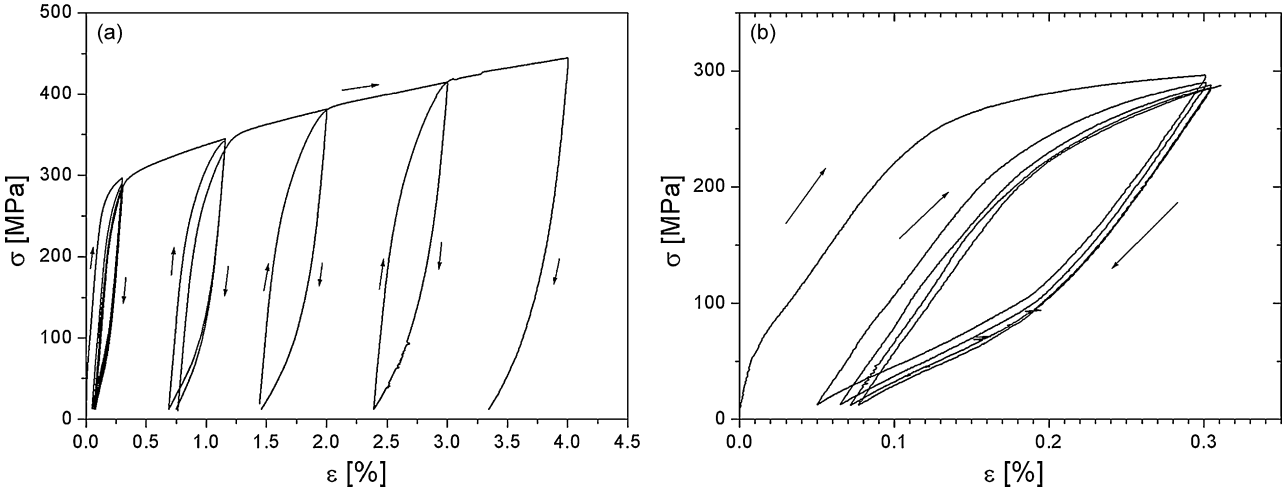

Fig. 3. (a) Tensile test at 100 °C. The sample was loaded and unloaded at different strain levels in order to study its pseudoelastic behavior. (b) Detailed view of the first series of cycles at ε = 0.3%.

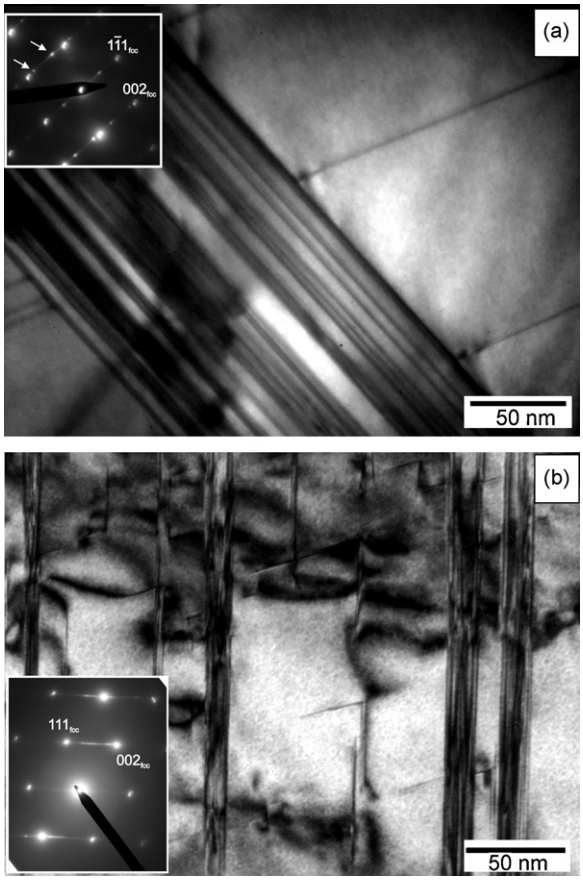

Fig. 4. (a) Bright field (BF) TEM image of a pre-rolled Fe–28Mn–6Si–5Cr (wt.%) sample tested at 100 °C. The inset shows the selected area diffraction (SAD) pattern, oriented accordingly. The zone axis is $[1\,1\,0]_{fcc}$. The SAD image has extra spots due to the presence of martensite, like those marked by arrows. The matrix is fcc while the plates containing lines with the darker contrast correspond to a mixture of hcp martensite and some isolated stacking faults. Individual dark lines are stacking faults in fcc. (b) BF TEM image of a sample deformed at room temperature. Martensite plates and stacking faults appear with a dark contrast in the figure. The zone axis is $[1\,1\,0]_{fcc}$. The SAD image has bright streaks related to the presence of a high density of stacking faults and an arrange of very thin martensite plates.

ture. The zone axis is $[1\,1\,0]_{fcc}$. This orientation allows observing martensite and stacking faults edge-on. Martensite can be recognized by the presence of extras spots in the SAD image (also shown as inset in Fig. 4a). In this picture, martensite appears as thin plates (about 5 nm wide), loosely grouped in bands together with stacking faults with the same orientation. This structure resembles what can be observed in samples where martensite was induced at room temperature and partially recovered by heating to high temperature [19]. In addition, there are a few stacking faults with a different orientation and the contrast of some dislocations superimposed to the martensite area. Fig. 4b shows the microstructure of a sample deformed at room temperature. The zone axis is also $[1\,1\,0]_{fcc}$, allowing a direct comparison with Fig. 4a. In this case, the microstructure shows several thin martensite plates, evenly distributed in the fcc matrix. This kind of microstructure has been shown and discussed in detail in Ref. [12]. The corresponding SAD image, shown as an inset in the figure, contains bright streaks. These streaks, usually related to the presence of stacking faults, also appear as a result of the morphology of the room temperature stress-induced martensite, i.e. extremely thin plates. This particular morphology is responsible for the large shape memory effect observed in this material [12]. Similar streaks are not present in the SAD image of the sample deformed at 100 °C (Fig. 4a), indicating that thinner hcp plates have transformed back to austenite.

TEM observations hint at the possible origin of the pseudoelasticity observed in this material. The accepted mechanism for the fcc/hcp transformation considers stacking faults in fcc as nucleation sites for the martensite [8]. At room temperature, the stacking fault energy (SFE) is low [14,20], so existing stacking faults are expected to be rather long and new ones are easy to nucleate. When external stress is applied on the samples, existing stacking faults grow by accumulating elastic tension around. When the tension reaches a certain limit, the material accommodates the associated strain either by introducing new stacking faults or perfect dislocations. As the SFE is low, the earlier is more probable. The subsequent formation of hcp martensite is a consequence of its relative stability and its direct formation mechanism. If stacking faults form on every second $\{111\}_{fcc}$ plane, instead of on every plane or every third plane for example, the material not only relieves the accumulated distortion but also forms a phase more stable than fcc consistent with the new existent stress conditions. The stress-induced martensite will then remain in the material until the temperature is raised above A_s. The material studied in this case has the additional characteristic of having a very large density of stacking faults, product of the pre-rolling thermomechanical treatment [12]. In consequence, it tends to form very thin martensite plates, evenly distributed in the matrix, because different stacking faults become active as the stress increases.

The increment of the test temperature to near 100 °C results in an increase of the SFE [14]. The stacking faults become shorter and their nucleation is more difficult. Under these conditions, the material reacts to the applied stress accommodating the deformation by elongating the existing stacking faults. Elastic tension again builds up near these growing faults. The main difference with the room temperature scenario is that, being the martensite less stable at this temperature, new stacking faults will not necessarily nucleate on every second $\{1\,1\,1\}_{fcc}$ plane. When that is the case, stable martensite plates form (Fig. 4) and remain there as long as the temperature is kept below A_s. However, there is an increased probability of new stacking faults nucleating on other planes. In such a case, they would act as new isolated stacking faults, i.e. growing under the application of stress and building up elastic distortion around. The introduction of irrecoverable slip also becomes more probable at higher temperature, a feature reflected in the observed decrease of the SME in similar materials under the same conditions [17]. Upon unloading, isolated stacking faults surrounded by elastic distortion shorten to recover their equilibrium length by moving backwards the limiting partial dislocations.

The macroscopic result of this process is the observed pseudoelasticity. As it was mentioned before, this particular material has a large density of stacking faults and in consequence, it displays a relatively pronounced pseudoelastic effect approximately up to point A (Fig. 3a). Based on this explanation, a certain degree of pseudoelastic behavior can be expected in most Fe–Mn-based alloys, due to their low SFE. However, the practical application of the effect would be restricted to a narrow temperature range (around 100 °C) and quite low deformation levels (about 0.4%).

4. Conclusions

We have studied the mechanical behavior of Fe–28Mn–6Si–5Cr (wt.%) shape memory alloy subjected to a simple thermomechanical treatment. Martensite can be stress-induced in this material up to 110 °C, while no martensitic transformation was detected at temperatures above 150 °C. The critical stress changes, first increasing with increasing temperature, and then decreasing above 110 °C. In the temperature range between 90 and 110 °C a relatively large pseudoelastic behavior has been observed consistent with the fact that martensite forms in this region. We propose that this pseudoe-

lasticity is due to the existence and formation of stacking faults and the reversible movement of their associated partial dislocations.

Acknowledgements

The authors gratefully acknowledge Pablo Riquelme and Carlos Talauer for their help in the preparation of samples for tensile tests.

References

[1] H. Otsuka, M. Murakami, S. Matsuda, MRS Int. Mtg. Adv. Mater. 9 (1989) 451–456.
[2] K.N. Melton, in: K. Otsuka, C.M. Wayman (Eds.), Shape Memory Materials, Cambridge University Press, Cambridge, 1998, pp. 223–224.
[3] H. Otsuka, H. Yamada, T. Maruyama, H. Tanahashi, S. Matsuda, M. Murakami, ISIJ Int. 30 (1990) 674–679.
[4] Z. Wang, J. Zhu, Mater. Sci. Eng. A 358 (2003) 273–278.
[5] K. Enami, A. Nagasawa, S. Nenno, Scripta Metall. 9 (1975) 941–948.
[6] A. Sato, E. Chishima, K. Soma, T. Mori, Acta Metall. 30 (1982) 1177–1183.
[7] A. Sato, E. Chishima, K. Soma, T. Mori, Acta Metall. 32 (1984) 539–947.
[8] S. Kajiwara, Mater. Sci. Eng. A 273–275 (1999) 67–88.
[9] N. Bergeon, S. Kajiwara, T. Kikuchi, Acta Mater. 48 (2000) 4053–4064.
[10] S. Kajiwara, D. Liu, T. Kikuchi, N. Shinya, Scripta Mater. 44 (2001) 2809–2814.
[11] A. Baruj, T. Kikuchi, S. Kajiwara, N. Shinya, Mater. Trans. 43 (2002) 585–588.
[12] A. Baruj, H.E. Troiani, Mater. Sci. Eng. A 481–482 (2008) 574–577.
[13] N.E. Stanford, D.P. Dunne, ISIJ Int. 46 (2006) 1703–1711.
[14] J. Wan, S. Chen, Curr. Opin. Solid State Mater. Sci. 9 (2005) 303–312.
[15] M. Sade, K. Halter, E. Hornbogen, J. Mater. Sci. Lett. 9 (1990) 112–115.
[16] H. Otsuka, K. Nakajima, T. Maruyama, Mater. Trans. JIM 41 (2000) 547–549.
[17] O. Matsumura, T. Sumi, N. Tamura, K. Sakao, T. Furukawa, H. Otsuka, Mater. Sci. Eng. A 279 (2000) 201–206.
[18] T. Sawaguchi, T. Kikuchi, S. Kajiwara, Smart Mater. Struct. 14 (2005) S317–S322.
[19] A. Baruj, T. Kikuchi, S. Kajiwara, Mater. Sci. Eng. A 378 (2004) 337–342.
[20] N.E. Stanford, K. Chen, D.P. Dunne, X.J. Jin, ISIJ Int. 47 (2007) 883–889.